
Meta-Learning the Search Distribution of Black-Box Random Search Based Adversarial Attacks

Maksym Yatsura
Bosch Center for Artificial Intelligence
University of Tübingen
maksym.yatsura@de.bosch.com

Jan Hendrik Metzen
Bosch Center for Artificial Intelligence
janhendrik.metzen@de.bosch.com

Matthias Hein
University of Tübingen
matthias.hein@uni-tuebingen.de

Abstract

Adversarial attacks based on randomized search schemes have obtained state-of-the-art results in black-box robustness evaluation recently. However, as we demonstrate in this work, their efficiency in different query budget regimes depends on manual design and heuristic tuning of the underlying proposal distributions. We study how this issue can be addressed by adapting the proposal distribution online based on the information obtained during the attack. We consider Square Attack, which is a state-of-the-art score-based black-box attack, and demonstrate how its performance can be improved by a learned controller that adjusts the parameters of the proposal distribution online during the attack. We train the controller using gradient-based end-to-end training on a CIFAR10 model with white box access. We demonstrate that plugging the learned controller into the attack consistently improves its black-box robustness estimate in different query regimes by up to 20% for a wide range of different models with black-box access. We further show that the learned adaptation principle transfers well to the other data distributions such as CIFAR100 or ImageNet and to the targeted attack setting¹.

1 Introduction

It was demonstrated that despite their impressive performance in various tasks, neural networks are susceptible to small imperceptible perturbations in the input called *adversarial examples* [4]. This is a concerning issue for real-world deployment of deep learning approaches, especially in safety-critical domains such as autonomous driving [5]. But apart from practical concerns, adversarial examples serve as a tool to better understand the true nature of artificial neural networks and capture their inherent properties and differences from their biological counterparts [6].

Evaluating adversarial robustness is usually formulated as a constrained optimization problem [4]. However, finding the exact solution is typically intractable [7, 8]. Therefore, in practice one often resorts to approximate methods called *adversarial attacks* that try to find adversarial examples within a small number of iterations. A number of different adversarial attacks were proposed [8–10] that can be distinguished into white- and black-box attacks. In white-box attacks, one assumes full access to the model architecture and weights [8]. However, as white-box attacks typically rely on the gradient, gradient obfuscation, which does not eliminate the existence of adversarial examples but makes it significantly harder to find them gradient-based, can be a severe obstacle for certain attacks [11].

¹The code is available at <https://github.com/boschresearch/meta-rs>

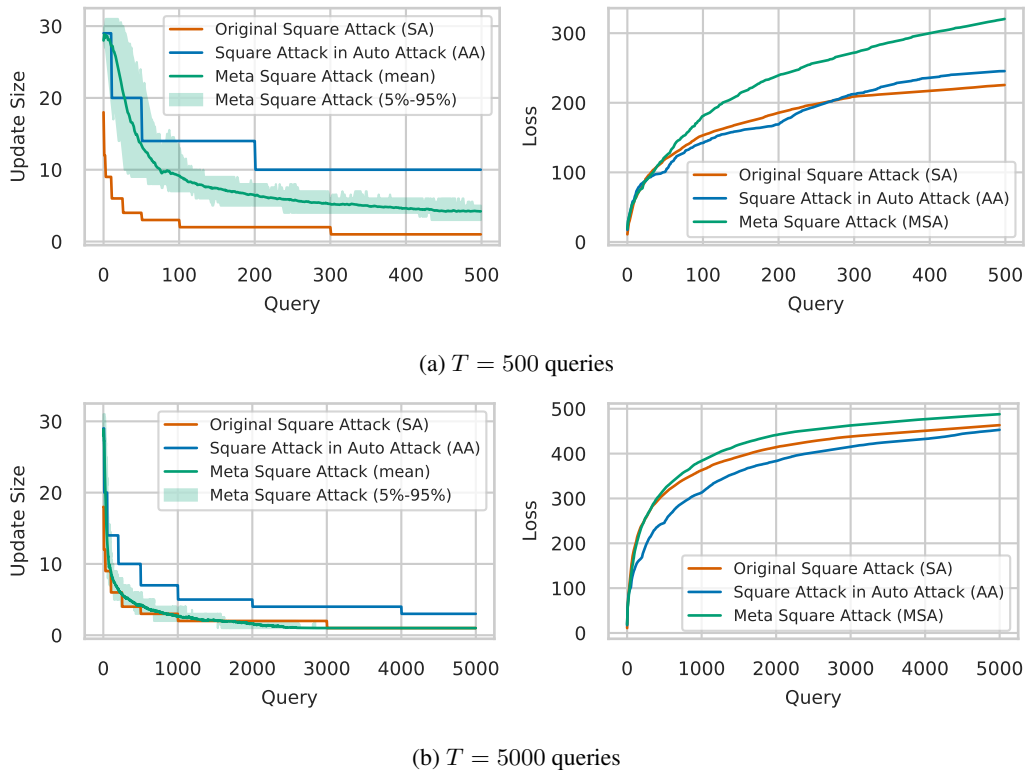


Figure 1: (Left) The schedules for SA [1] (which scales accordingly for different query budgets) and AA [2] compared to Meta Square Attack (MSA) proposed in this work. MSA adapts the update size during the course of the attack for each image. We illustrate the mean and the percentile range for a given set of attacked images. (Right) The maximization of the loss for the model of Ding et al. [3] on 100 CIFAR10 images. MSA outperforms SA and AA significantly in terms of the achieved loss.

Therefore, black-box attacks that use only limited information from the model such as the class scores or the final decision often provide an additional perspective on the true robustness of the model [12–21] and are thus recommended for reliable robustness evaluation [2, 22].

A very promising direction in the field of black-box adversarial attacks are randomized search schemes for crafting adversarial examples [1, 23, 24]. Combining random search with specific update proposal distributions allows to achieve state-of-the-art black-box efficiency for different threat models such as ℓ_∞ and ℓ_2 [1], ℓ_1 [25], ℓ_0 , adversarial patches, and adversarial frames [24]. Despite the conceptual simplicity of these methods, the main disadvantage of random search based methods is that the construction of a suitable proposal distribution requires significant manual design and is crucial for competitive performance (see also Figure 1).

In this work, we propose a method that allows to circumvent the fine-tuning and reduce the amount of manual design in random search based attacks. We use gradient-based meta-learning to automatically optimize controllers for schedules and proposal distribution on models with white-box access. After meta-training, the controllers can be plugged into a random search attack substituting manually designed schedules and proposal distributions. Importantly, once meta-trained, the controllers do not require any gradient access and can thus be used in a fully black-box setting and without being affected by gradient obfuscation. We consider the proposed methodology for the case of Square Attack for the ℓ_∞ and ℓ_2 threat models [1]. We meta-train controllers for update size and color on an adversarially trained [26] ResNet18 [27] model with white-box access and apply them to many different models from the RobustBench model zoo [28] that we treat as black-boxes. Since query efficiency is of crucial importance in black-box adversarial attacks, we also study the method for different query regimes ranging from several hundreds to several thousands. Depending on the query regime and the attacked model we obtain up to 20% improvement with respect to the baseline schedules proposed by Andriushchenko et al. [1] and Croce and Hein [2].

In short, we make the following contributions:

- We frame adversarial attack optimization as a meta-learning problem (Section 3.2).
- We formalize the gradient-based meta-learning for the state-of-the-art Square Attack and propose Meta Square Attack (Section 3.3).
- We meta-train Meta Square Attack (MSA) on a CIFAR10 [48] model with white-box access and show that MSA improves robust accuracy by up to 5.6% on a vast range of CIFAR10 models with black-box access with respect to the hand-designed search distributions proposed in previous work [1, 2] for the ℓ_∞ and ℓ_2 threat models (Section 4).
- We show that Meta Square Attack generalizes well to different datasets and to the targeted attack setting. It achieves up to 20% better robust accuracy compared to the state-of-the-art baseline [1] for attacking models on CIFAR100 and ImageNet (Section 4.2).

2 Related Work

Black-box adversarial attacks: Existing approaches to black-box robustness evaluation can be divided into several groups based on their mode of interaction with the target model. Transfer-based attacks [17, 29] rely on having a model with white-box access that is similar to the targeted model. If this is the case, one can generate adversarial perturbations for this substitute model and transfer them in a black-box setting. A downside of such approaches is that similarity between the models is a crucial factor. Without it the efficiency of transfer attacks is drastically reduced [29]. Decision-based attacks [13, 20, 30] applied to classifiers assume that one can submit queries to the model and receive the predicted class label. Score-based attacks [1, 12–19] consider broader access to the model and assume the attack receives predicted scores for all the classes. Prior work [15, 31, 32] use this information to estimate a gradient and apply gradient descent. Alzantot et al. [19] propose a derivative-free approach based on genetic algorithms. Several works use the empirical observation that successful ℓ_∞ perturbations are located at the corners of the color cube, therefore instead of continuous optimization one can reduce the problem to a discrete one [1, 12, 24, 33].

Meta-learning and adversarial robustness: The closely related fields of meta-learning [34] and learning to optimize [35] have been employed in the field of adversarial robustness. The idea of learned optimizers [36, 37] was applied to finding adversarial examples in white-box [38] and black-box [39] settings. Meta-learning [40, 41] was also used to improve zeroth-order gradient estimation and allow better query efficiency of black-box attacks [42]. Besides that there is the recent work [43] on automating the existing AutoAttack [2] framework for robustness evaluation. Meta-learning has also been used as part of adversarial training [38, 44] for increasing adversarial robustness.

Square Attack: Square Attack (SA) was proposed by Andriushchenko et al. [1] and combines classical random search with a heuristic design of the update rule. This design depends on the geometry of the perturbation set and therefore differs for ℓ_∞ - and ℓ_2 -attacks and was later extended also to ℓ_1 [25]. As the adversarial attack problem is highly non-convex, a good initialization can significantly improve query efficiency. SA uses a stripe initialization motivated by empirical findings [45]. The design principle of the attack is based on the observation that the strongest perturbations are usually found on the boundary of the feasible set [18]. For the ℓ_∞ -case, updates are sampled as squares parametrized by square size, square color, and position of the square. Performance of SA depends heavily on how color, position, and square size are chosen, which requires manual design.

The square size schedules employed by previous work are relatively sophisticated (indicating non-trivial manual design): Andriushchenko et al. [1] proposed a schedule parametrized by $p^0 \in [0, 1]$ (the fraction of image pixels to be modified by a square in the first query) and the total query budget T , where p^t is halved at $\{0.1, 0.5, 2, 10, 20, 40, 60, 80\}\%$ of the total query budget. For evaluation on CIFAR10, Andriushchenko et al. [1] suggest different values of p^0 and report $p^0 = 0.3$ as a default choice. Croce and Hein [2] proposed a different schedule for SA to be used in AutoAttack: they use $p^0 = 0.8$ and $T = 5000$ but fix the halving points of p^t as if $T = 10000$. An illustration of the two schedules for $T = 500$ and $T = 5000$ can be seen in Figure 1.

The second aspect that characterizes SA is the distribution from which position and color of the next square are sampled. For positions, the distribution is uniform over all positions for which a square of a given size would be fully contained in the input. For colors, SA always generates points on the boundary of the perturbation set (corners of the color cube) and uses a uniform distribution over the 2^c different colors (with c being number of channels, typically $c = 3$).

Thus SA either relies on extensive manual design (for the square size schedules) or resorts to simple baseline choices (such as the uniform distributions over colors and positions) which might be suboptimal. In this work, we show that meta-learning SA consistently improves the already strong performance of SA (see Section 4.2) with very little manual design and identify non-trivial patterns that increase attack efficiency (see Section 4.3).

3 Method

In the following, we briefly introduce the formulation of the optimization problem for an adversarial attack, rephrase it in the form of a meta-learning problem, and introduce our method for learning the search distribution of a specific random search based black-box adversarial attack, namely Square Attack [1]. We denote this method as Meta Square Attack (MSA).

3.1 Adversarial Robustness Evaluation

Let K be the number of classes in a classification problem and $f : [0, 1]^d \rightarrow \Delta^{K-1}$ be a classifier which maps a d -dimensional input x to

$$\Delta^{K-1} = \left\{ (p_0, \dots, p_{K-1}) \in \mathbb{R}^K \mid \sum_{i=0}^{K-1} p_i = 1, \text{ and } p_i \geq 0 \text{ for } i = 0, \dots, K-1 \right\},$$

which denotes the set of probability distributions over the K discrete possible outcomes. For a label $y \in \{0, \dots, K-1\}$, a loss function $l : \Delta^{K-1} \times \{0, \dots, K-1\} \rightarrow \mathbb{R}$, a perturbation set S , and operator a , we define the robustness evaluation problem as:

$$V(f, x, y) = \max_{\xi \in S} l(f(a(x, \xi)), y) \quad (1)$$

For $S = \{\xi \mid \|\xi\|_p \leq \epsilon\}$ and $a(x, \xi) = \Pi_{[0,1]^d}(x + \xi)$ (where $\Pi_{[0,1]^d}$ is the projection onto $[0, 1]^d$), one obtains the standard ℓ_p ball threat model for images. Assuming that the loss function l and operator a are fixed, we denote $L(f, x, y, \xi) := l(f(a(x, \xi)), y)$ as a functional that one needs to maximize in robustness evaluation.

Since exact maximization of Equation (1) is intractable in the general case [7], we consider a (potentially non-deterministic) procedure $\mathcal{A}_\omega(L, f, x, y)$ called adversarial attack. This attack \mathcal{A}_ω is parametrized by hyperparameters ω and designed with the intention that $\xi^\omega \sim \mathcal{A}_\omega(L, f, x, y)$ with $\xi^\omega \in S$ becomes an approximate solution (tight lower bound) of $V(f, x, y)$, that is $V(f, x, y) - L(f, x, y, \xi^\omega)$ should become small (in expectation). Optimizing the hyperparameters of the attack via $\max_{\omega} \mathbb{E}_{\xi^\omega \sim \mathcal{A}_\omega(L, f, x, y)} L(f, x, y, \xi^\omega)$ can allow a tighter lower bound of $V(f, x, y)$. Unfortunately, this maximization is still intractable typically, for instance when f is a black-box (no gradient information is available), the number of queries to f per data (x, y) is limited, or \mathcal{A}_ω has high variance.

3.2 Black-box Adversarial Attack Optimization as a Meta-learning Problem

We now frame optimization of the adversarial attack in the query-restricted black-box setting as a *meta-learning* problem. We follow the taxonomy proposed in the recent survey on meta-learning by Hospedales et al. [34].

First, we formulate our **meta-objective** (the specification of the goal of meta-learning): we assume data to be governed by a distribution $(x, y) \sim \mathcal{D}$ and classifiers defined on this data, which need to be evaluated, by a distribution $f \sim \mathcal{F}$. Our meta-objective is to find parameters ω^* of the attack \mathcal{A}_ω that maximize the lower bound $L(f, x, y, \xi^\omega)$ of $V(f, x, y)$ in expectation across models $f \sim \mathcal{F}$, data $(x, y) \sim \mathcal{D}$, and the stochastic attack $\xi^\omega \sim \mathcal{A}_\omega$:

$$\omega^* = \operatorname{argmax}_{\omega} \mathbb{E}_{f \sim \mathcal{F}} \mathbb{E}_{(x, y) \sim \mathcal{D}} \mathbb{E}_{\xi^\omega \sim \mathcal{A}_\omega(L, f, x, y)} L(f, x, y, \xi^\omega) \quad (2)$$

Here, the expensive optimization of ω^* is amortized across models and data. More specifically, we assume finite sets of data $D = \{(x_i, y_i)_{i=1}^N \mid (x_i, y_i) \sim \mathcal{D}\}$ and classifiers $F = \{f_j \mid f_j \sim \mathcal{F}\}$

are available. Moreover, we assume the $f_j \in \mathcal{F}$ allow white-box access and quasi-unrestricted number of queries. The sets D and F can be used during *meta-training* of the attack, that is the objective during meta-training becomes $\omega^* = \arg \max_{\omega} R(F, D, \omega)$ with $R(F, D, \omega) = \sum_{f \in F} \sum_{(x,y) \in D} L(f, x, y, \xi^\omega)$ and $\xi^\omega \sim \mathcal{A}_\omega(L, f, x, y)$. However, the ultimate goal of meta-learning is to apply \mathcal{A}_{ω^*} during *meta-testing* to unseen $(x, y) \sim \mathcal{D}$ and unseen $f \sim \mathcal{F}$ that allow only black-box and query-limited access, and maximize $\mathbb{E}_{\xi^\omega \sim \mathcal{A}_\omega(L, f, x, y)} L(f, x, y, \xi^\omega)$, that is: the attack needs to generalize across models and data.

Next, we define the **meta-representation**, that is how the adversarial attack \mathcal{A}_ω is designed and parametrized such that generalization across $f \sim \mathcal{F}$ is effective. In this work we focus on random search based adversarial attacks for black-box robustness evaluation since they have achieved strong results in prior work and are amenable to meta-learning. Let \mathcal{A}_ω be a random search based attack with a query budget limited by T . Then an adversarial perturbation $\xi^\omega = \xi^T \sim \mathcal{A}_\omega(L, f, x, y)$ is obtained using the following iterative procedure:

$$\xi^0 \sim \mathcal{D}^0; \quad \xi^{t+1} = \underset{\xi \in \{\xi^t, \Pi_{\mathcal{S}}(\xi^t + \delta^{t+1})\}}{\operatorname{argmax}} L(f, x, y, \xi); \quad \delta^{t+1} \sim \mathcal{D}_\omega(t, \xi^0, \delta^0, \dots, \xi^t, \delta^t), \quad (3)$$

where $\Pi_{\mathcal{S}}$ corresponds to the projection onto the perturbation set \mathcal{S} .

That is, we assume a fixed distribution \mathcal{D}^0 for initializing the perturbation ξ^0 but a meta-learnable \mathcal{D}_ω for the update proposals δ^{t+1} . Importantly, \mathcal{D}_ω depends on the entire attack trajectory up to step t . Since this trajectory contains implicitly information on the classifier f when applied to data (x, y) , our meta-learned random search attack can adapt to the classifier and data at hand. We provide more details on \mathcal{D}_ω for the specific case of Square attack [1] in Section 3.3.

The **meta-optimizer** (how we optimize the meta-objective) in our case assumes that both the loss function l and \mathcal{A}_ω are (stochastic) differentiable with respect to ω or we can find differentiable relaxations (as we will discuss in Section 3.3). Thus the meta-parameters ω can be optimized using stochastic gradient descent on mini-batches $B \subseteq D$ based on the (stochastic) gradient

$$g = \nabla_{\omega} R(F, D, \omega) = \sum_{f_j \in F} \sum_{(x_i, y_i) \in B \subseteq D} \nabla_{\omega} L(f_j, x_i, y_i, \xi_{i,j}), \quad (4)$$

where $\xi_{i,j} \sim \mathcal{A}_\omega(L, f_j, x_i, y_i)$. However, due to the stochasticity of \mathcal{A}_ω induced by \mathcal{D}^0 and \mathcal{D}_ω , the discrete argmin in the update step of \mathcal{A}_ω , and the length T of the unrolled optimization (often in the order of hundreds to thousands queries), g would have very high variance and typically one would also face issues with vanishing or exploding gradients. To address this, we propose using a greedy alternative instead:

$$g = \frac{1}{T} \sum_{f_i} \sum_{(x_j, y_j)} \sum_{t=1}^{T-1} \nabla_{\omega} L(f_i, x_j, y_j, \Pi_{\mathcal{S}}(\xi^t + \delta^{t+1})). \quad (5)$$

Importantly, even though ξ^t depends on ω for $t > 0$, we do not propagate gradients with respect to ω through ξ^t , that is we set $\nabla_{\omega} \xi^t := 0$. By this, the gradient corresponds to optimizing \mathcal{D}_ω in a myopic way, such that proposals $\delta^{t+1} \sim \mathcal{D}_\omega(t, \xi^0, \delta^0, \dots, \xi^t, \delta^t)$ are trained to maximally increase the immediate loss in step $t + 1$. While this introduces a bias of acting myopic and greedy, it works reasonably well in practice.

We can now rewrite $\nabla_{\omega} L(f_i, x_j, y_j, \xi^t + \delta^{t+1}) = \nabla_{\delta^{t+1}} L(f_i, x_j, y_j, \xi^t + \delta^{t+1}) \nabla_{\omega} \delta^{t+1}$. We note that $\nabla_{\omega} \delta^{t+1}$ can be a very high variance estimate of $\nabla_{\omega} \mathcal{D}_\omega(t, \xi^0, \delta^0, \dots, \xi^t, \delta^t)$ depending on the stochasticity of \mathcal{D}_ω . However, as it is an unbiased estimate and we average over very many steps T and models and data, g is still a sufficiently good estimate in practice.

3.3 Meta Square Attack

In this section, we demonstrate how the proposed meta-learning approach can be applied to Square Attack (SA) [1] with ℓ_∞ threat model. We denote the resulting meta-learned attack as *Meta Square Attack* (MSA). We keep \mathcal{D}^0 as the stripe initialization from SA and focus on meta-learning \mathcal{D}_ω as it governs all but the first step. As discussed in Section 2, sampling $\delta^{t+1} \sim \mathcal{D}(t)$ in SA proceeds by computing a square size (its width in pixels) $s_t = \pi^s(t) \in \{1, \dots, s_{max}\}$ and sampling a

position $(p_x, p_y) \sim \pi^p(s) \in \{1, \dots, s_{max} - s\}^2$ and a color $c \sim \pi^c \in \{c_1, \dots, c_m\}$. In SA, π^s is a heuristic schedule that depends on t (and differs in prior work [1, 2]) and both π^p and π^c are uniform distributions. δ^{t+1} is then chosen to be zero everywhere except for a square of size s at position p with color c . Possible colors c_i correspond to the eight corners of the RGB hypercube with ℓ_∞ norm ϵ . That is $c_i \in (\pm\epsilon, \pm\epsilon, \pm\epsilon)$, while s_{max} is chosen maximally with the constraint that all sampled squares must not exceed the image dimensions. We keep π^p as uniform distribution, but meta-learn the controllers $\pi_{\omega_s}^s$ and $\pi_{\omega_c}^c$ with parameters $\omega = (\omega_s, \omega_c)$.

Update size controller $\pi_{\omega_s}^s$. We design $\pi_{\omega_s}^s$ as a multi-layer perceptron (MLP) with parameters ω_s . The MLP outputs a scalar value $s' \in \mathbb{R}$ and we map this value to the actual update size via $s = \sigma(s') \cdot (s_{max} - 1) + 1$ with $\sigma(x) = 1/(1 + e^{-x})$. During meta-testing, we round the continuous $s \in [1, s_{max}]$ to a discrete value $\lfloor s \rfloor \in \{1, \dots, s_{max}\}$. As this would block gradient flow during meta-training, we relax the square sampling in SA such that it supports continuous update sizes. The details of this relaxed sampling can be found in the Appendix A.3. Importantly, it is only conducted during meta-training and not in the final evaluation during meta-testing.

We provide two scalar inputs to the MLP $\pi_{\omega_s}^s$: (a) the current query t encoded as $\log_2(\frac{t}{T} + 1)$ where T is the maximal number of queries. It ensures that the input stays in the range $[0, 1]$ for $t \leq T$. We use $T = 5000$. (b) Let $r^{t+1} = H(L(f, x, y, \Pi_S(\xi^t + \delta^{t+1})) - L(f, x, y, \xi^t)) \in \{0, 1\}$ be an indicator of whether adding δ^{t+1} at time $t + 1$ improved the loss (for H being the Heaviside step-function). The MLP gets as second input at time t the value $R^t = \gamma R^{t-1} + (1 - \gamma)r^t/r^0$ with $R^0 = 1$. Here γ is a decay term that controls how quickly past experience is “forgotten” and $r^0 = 0.25$ is a constant whose purpose is to ensure that the MLP’s second input has a similar scale as the first (namely in $[0, 1]$). Intuitively, (a) allows to schedule update sizes based on time step of the attack (this information is also used in SA itself) while (b) allows adapting the update size based on the recent success frequency R^t of proposals (for instance reducing the update size if few proposals were successful recently). Thus (b) allows the schedule to adapt to classifier f and data (x, y) at hand.

Color controller $\pi_{\omega_c}^c$. We design the color controller $\pi_{\omega_c}^c$ as a categorical distribution $c^t \sim \text{Cat}(\alpha_1^t, \dots, \alpha_m^t)$, where each $\alpha_i^t \in \mathbb{R}$ is predicted by an MLP with weights ω_c . The m MLPs for the α_i^t share weights ω_c but differ in their inputs. In order to differentiate through the categorical distribution at meta-train time, we reparametrize the categorical distribution with Gumbel-softmax and draw discrete (hard) samples in the forward pass but treat them as soft samples in the backward pass [46, 47]. Additionally, we ensure that every color c_i is sampled at least with probability p_{min}^c by assigning $P(c_i) = p_{min}^c + (1 - mp_{min}^c)P_{\text{Cat}(\alpha_1^t, \dots, \alpha_m^t)}(c_i)$. This ensures continuous exploration of all m colors.

The m MLPs get two inputs: (a) the current query t encoded as $\log_2(\frac{t}{T} + 1)$ (same encoding as for the step size controller and also same for all m MLPs). (b) Information regarding the recent success frequency of proposals δ^t based on squares of the respective colors ($c^t = c_i$):
$$R_i^t = \begin{cases} \gamma R_i^{t-1} + (1 - \gamma)r^t/r^0 & \text{if } c^t = c_i \\ R_i^{t-1} & \text{otherwise} \end{cases}.$$
 This second input allows the controller to learn, e.g., to sample those colors more often that resulted in higher success frequency recently.

4 Experiments

We perform an empirical evaluation of Meta Square Attack (MSA). First, we consider the data distribution \mathcal{D} of CIFAR10 [48] images and a classifier distribution \mathcal{F} consisting of the classifiers robust with respect to the ℓ_∞ -threat model. We use this setting for the meta-training as discussed in Section 4.1. We further consider how the controllers trained for these distributions generalize to working with the other data distributions of CIFAR100 and ImageNet and corresponding distributions of classifiers defined on this data. We also discuss the meta-training for the distribution of the classifiers robust with respect to the ℓ_2 -threat model in the Section A.5.

We compare the performance of MSA in 4 different query budget regimes to manually designed schedules for Square Attack proposed by Andriushchenko et al. [1] (denoted by SA) and Croce and Hein [2] (denoted by AA). The reason why we have chosen this evaluation mode instead of reporting accuracy and average number of queries for some single fixed budget is that the original SA approach proposes to scale the schedule to a given budget (Figure 1). Hence, it uses the knowledge of the attack budget and the schedule used for 500 queries is not a truncated version of the schedule used for

Table 1: MSA compared to SA [1] and AA [2] in the ℓ_∞ -threat model with $\epsilon = 8/255$ on 1000 CIFAR10 test images. We report mean and standard error of robust accuracy across 5 runs with different random seeds. The full results for 16 CIFAR10 models can be found in Table 8.

Model	Accuracy (%)		Attack	Query budget			
	Clean	Robust		500	1000	2500	5000
Wong et al. [51]	83.34	43.21	SA	69.7±0.15	63.5±0.10	55.1±0.04	50.8±0.08
			AA	69.5±0.21	63.9±0.10	57.4±0.07	53.6±0.06
			MSA	63.9±0.12	59.1±0.09	53.0±0.16	49.8±0.08
Huang et al. [52]	83.48	53.34	SA	72.3±0.10	66.6±0.16	60.5±0.09	57.3±0.08
			AA	70.6±0.10	66.5±0.07	61.2±0.10	58.5±0.11
			MSA	66.1±0.10	62.9±0.15	58.7±0.05	56.8±0.08

5000 queries as it is done in AA. Since adapting the schedule to different query budgets is a crucial factor for the manually designed schedules that we consider as baselines, we choose the evaluation regime that allows to take this factor into consideration. Section 4.2 summarizes the experimental results (for more details see the Section A.1 in the Appendix) and Section 4.3 analyzes the behavior learned by the controllers.

4.1 Meta-Training and Controller Design

We meta-train the controller on a single robust model $f \sim \mathcal{F}$ with white-box access (the “source model”). The source model was designed such that attackers could easily and cheaply acquire it themselves: the model has ResNet18 [27] architecture and was trained on the CIFAR10 training set using adversarial training [26] with the advtorch [49] package. Adversarial training was done using ℓ_∞ -PGD attack with $\epsilon = 8/255$, fixed step size of 0.01, and 20 steps.

For both update size and color controllers, we use MLP architectures with 2 hidden layers, 10 neurons each, and ReLU activations. We purposefully did not finetune the MLP architecture. Meta-training was run on a set D consisting of 1000 images from CIFAR10 test set (different from the ones used in evaluation of controllers in the next subsection) and Square Attack with a query budget of 1000 iterations. Therefore, controller behaviour on query regimes higher than 1000 are obtained by extrapolation of the behaviour learned for 1000 iterations. Both controllers were trained simultaneously for 10 epochs using Adam optimizer with batch size 100 and cosine step size schedule [50] with learning rate 0.03. The total loss improvement over the attack was used as meta-loss that we optimized in meta-training. We always run the attack on all images for the full budget T , since removing images from the attacked batch would cause discontinuity in the meta-loss. All computations including meta-training and evaluation of the controllers were performed on a single Nvidia Tesla V100-32GB GPU.

4.2 Evaluation

In this section, we evaluate how the Meta Square Attack (MSA) obtained by training on a CIFAR10 model with white-box access discussed in the Section 4.1 performs for different models and datasets.

Table 1 illustrates that MSA transfers well to two selected robust CIFAR10 models. Moreover, Table 2 reports results aggregated over a broad range of 16 robust CIFAR10 models from RobustBench (see Table 8 in the Appendix A.4 for details). We report mean, minimal, and maximal improvement across all the 16 models. We observe a consistent improvement for each considered query budget regime, which is especially pronounced for lower query regimes of 500 and 1000 queries. The improvements generalize to a budget of 5000 queries, which is five times higher than the one used during meta-training.

As described in Section 3.3, the input to MSA_s and MSA_c is not specific to the data distribution. Therefore, we also show that the adaptation principles learned on a CIFAR10 model transfer well to attacking models that not only have different architecture but also operate on significantly different

²Meta-training on more than one source model could improve generalization across models, but we found that even meta-training on a single model generalizes sufficiently well.

Table 2: Improvement in l_∞ -robust accuracy of our MSA with respect to the *best* of the previous Square Attack configurations, SA [1] and AA [2], in the setting of Table 1. The results are accumulated across 16 robust CIFAR10 models from RobustBench [28] (see Table 8 for full results).

Query budget	500			1000			2500			5000		
Improvement in	mean	min	max	mean	min	max	mean	min	max	mean	min	max
robust accuracy (%)	4.29	3.1	5.6	3.87	2.7	5.4	1.63	0.9	2.1	0.38	-0.1	1.0

Table 3: **Transfer to CIFAR100:** MSA trained on a CIFAR10 model consistently outperforms SA [1] and AA [2] on CIFAR100 (1000 images) in robust accuracy for the l_∞ -threat model with $\epsilon = 8/255$. Averaged across 3 runs with different random seeds.

Model	Accuracy (%)		Attack	Query budget			
	Clean	Robust		500	1000	2500	5000
Wu et al. [53]	60.38	28.86	SA	43.3±0.17	38.7±0.09	33.9±0.28	32.3±0.20
			AA	41.3±0.20	37.6±0.00	35.0±0.06	32.7±0.35
			MSA	37.8±0.07	35.5±0.12	33.1±0.03	32.2±0.03
Cui et al. [54]	70.25	27.16	SA	48.9±0.03	42.3±0.20	33.6±0.09	30.5±0.06
			AA	47.5±0.17	42.8±0.09	35.9±0.13	32.5±0.15
			MSA	42.6±0.13	37.8±0.12	32.5±0.30	30.1±0.09

data distributions: Table 3 demonstrates generalization of the learned controllers for attacking robust models for CIFAR100 [48]. We also consider the transfer to ImageNet [57] dataset that has significantly higher input dimension and number of classes than CIFAR10. In Table 4, one can see that MSA significantly improves the results even in the high extrapolation regime of 5000 queries. We also observe considerable improvement of the robust accuracy estimate for the targeted attacks on undefended ImageNet models (Table 5). Results for applying the size controller trained specifically for the l_2 threat model (together with the color controller trained for l_∞) are in Table 6. We observe consistent improvement of about 3% robust accuracy for all of the considered query budgets. The magnitude of improvement for different datasets and threat models depend on two factors: how well the adaptation mechanism learned by our controllers generalizes in the given setting and how suitable the hand-designed search distributions of the baselines [1, 2] are for each particular problem. The consistency of the improvement indicates that the adaptive search distribution makes Meta Square Attack more efficient in the majority of the settings.

4.3 Analysis of Learned Controllers

As the learned controllers are black-boxes (implemented by MLPs), it may be non-trivial to understand their realized strategy. We present some analysis of the controllers’ internal strategy based on their empirical behavior. Further analysis can be found in the Section A.4.

Table 4: **Transfer to ImageNet:** MSA trained on a CIFAR10 model consistently outperforms SA [1] and AA [2] on 1000 ImageNet validation set images in l_∞ -robust accuracy for $\epsilon = 4/255$. For SA we use $p^0 = 0.05$ as in Andriushchenko et al. [1]. Averaged across 3 different runs.

Model	Accuracy (%)		Attack	Query budget			
	Clean	Robust		500	1000	2500	5000
resnet18 Salman et al. [55]	52.5	25.0	SA	50.6±1.43	48.1±1.18	43.9±1.00	40.3±1.21
			AA	45.2±1.09	43.5±0.86	41.0±1.07	39.0±1.21
			MSA	43.3±1.00	41.7±0.94	39.1±1.23	37.8±1.36
resnet50 Engstrom et al. [56]	63.4	27.6	SA	59.8±0.64	57.2±0.79	52.9±1.11	48.6±1.31
			AA	54.6±0.99	52.8±1.09	50.3±1.43	48.1±1.18
			MSA	52.5±1.23	50.8±1.47	48.0±1.15	45.8±1.35

Table 5: MSA trained on a CIFAR10 model attacking the **undefended ImageNet models** in the ℓ_∞ threat model with $\epsilon = 0.05$. We compare our method with SA and set $p^0 = 0.05$ for the untargeted case and $p^0 = 0.01$ for the targeted case as suggested by Andriushchenko et al. [1]. For the targeted attacks robust accuracy is the fraction of the total number of images that was initially correctly classified by the model and not shifted to the target class during the attack. We provide clean accuracy of the models on a subset of 1000 ImageNet validation set images that we consider.

Model	Clean acc. (%)	Attack	Untargeted				Targeted			
			500	1000	2500	5000	500	1000	2500	5000
ResNet-50 [58]	77.3	SA	8.8	5.1	0.2	0.0	76.9	75.1	62.5	34.4
		MSA	2.9	0.8	0.0	0.0	67.1	52.0	27.8	12.1
VGG-16-BN [59]	75.0	SA	2.8	0.9	0.0	0.0	74.5	72.2	51.5	17.4
		MSA	1.8	0.2	0.0	0.0	62.5	45.2	16.5	3.5
Inception v3 [60]	77.6	SA	16.6	6.1	2.3	1.0	77.5	76.4	70.9	59.8
		MSA	10.2	5.1	2.6	1.3	74.4	70.6	60.1	49.5

Table 6: ℓ_2 -threat model: MSA₂ uses the update size controller trained for the ℓ_2 attack on a CIFAR10 model (see Section 4.1). The color controller is the same as for the ℓ_∞ case. ℓ_2 -MSA outperforms consistently ℓ_2 -SA [1] and ℓ_2 -AA [2] in terms of ℓ_2 -robust accuracy for $\epsilon = 0.5$ on 1000 CIFAR10 images. The full results for 5 models can be found in the Table 10.

Model	Accuracy (%)		Attack	Query budget			
	Clean	Robust		500	1000	2500	5000
Ding et al. [3]	88.02	66.09	SA	85.5±0.06	83.9±0.18	81.1±0.00	78.7±0.06
			AA	82.8±0.09	81.4±0.06	79.3±0.07	77.6±0.09
			MSA ₂	82.3±0.03	80.9±0.07	77.4±0.09	75.8±0.19
Rice et al. [61]	88.67	67.68	SA	86.3±0.07	84.7±0.10	81.4±0.26	79.7±0.07
			AA	83.7±0.12	81.4±0.09	79.9±0.09	78.6±0.18
			MSA ₂	82.6±0.09	81.0±0.07	78.7±0.03	76.9±0.25

Figure 2a illustrates the behaviour of the update size controller MSA_s. It shows how the controller chooses the update size over time in an artificial scenario where the success probability $P(r^t = 1)$ is modeled to be constant. As implemented also by the heuristic schedules SA and AA, update size decays over time. However, the decay pattern depends heavily on $P(r^t = 1)$, with slower decay for larger $P(r^t = 1)$. This property is not implemented by heuristic schedules, but makes sense intuitively: high $P(r^t = 1)$ corresponds to a situation where the current perturbation ξ^t can be improved relatively easily by coarse-grained changes implemented by the current update sizes; in this case it makes sense to first get the coarse-grained structure "right", before proceeding to fine-grained details that can be captured by small squares.

Figure 2b illustrates the empirical behavior of the color controller MSA_c when attacking the model by Ding et al. [3]. Shown are histograms over 500 images for the frequency of specific colors being sampled up to the respective iteration. Prior work like SA and AA maintained a uniform distribution of colors. However, the learned controller shows a clear preference for sampling black and white more often than uniform ($p \approx 0.18$ vs. $p = 0.125$ for uniform), blue and yellow approximately with $p = 0.125$, and the other colors less often than uniform. Since the color controller depends on the success rates R^t of colors, this behavior is not hard-coded into the controller but identified on-the-fly during the attack (so behavior can differ for models with different vulnerabilities).

Table 7 demonstrates the ablation studies with respect to the used controllers on the model by Goyal et al. [62]. We observe that MSA_s combined with the uniform color distribution alone significantly improves the results of SA and AA in most of the query budgets (with the exception of the strong extrapolation regime of 5000 queries). The controller MSA_c combined with all schedules improves the performance with the exception of 500 queries regime for SA and MSA_s where it provides an equal or a slightly worse result in some cases.

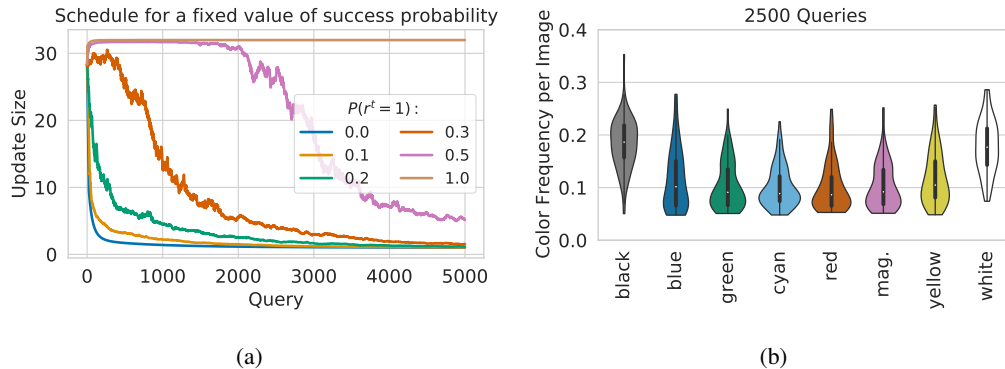


Figure 2: (a) Square-size schedule obtained from MSA_s over time for fixed values of success probability $P(r^t = 1)$ (averaged over 25 runs) (b) Illustration of color frequency histogram of 500 images after 2500 queries of MSA_c .

Table 7: We compare the update size controller MSA_s to the schedules from SA [1] and AA [2] in the ℓ_∞ threat model with $\epsilon = 8/255$ on a model by Gowal et al. [62] with 1000 CIFAR10 test images. We also compare the uniform color sampling to our color controller MSA_c . Averaged across 5 runs with different random seeds.

Update size schedule	Color sampling	Query budget			
		500	1000	2500	5000
SA	Uniform	80.6±0.09	76.7±0.07	70.8±0.14	67.5±0.07
SA	MSA_c	81.0±0.05	76.4±0.08	69.9±0.10	67.2±0.07
AA	Uniform	80.0±0.17	76.8±0.11	72.2±0.10	69.2±0.08
AA	MSA_c	79.9±0.12	76.7±0.03	71.6±0.17	68.8±0.07
MSA_s	Uniform	76.9±0.05	73.7±0.05	69.8±0.13	67.6±0.04
MSA_s	MSA_c	76.9±0.07	73.4±0.13	69.0±0.08	67.2±0.04

5 Conclusion

In this work we propose a theoretical framework for meta-learning search distributions that help to improve efficiency of random search based black-box adversarial attacks. We implement and investigate this framework for Square Attack with ℓ_∞ and ℓ_2 perturbations. Our experimental results show that learned adaptive controllers improve attack performance across different query budgets and generalize to new datasets as well as targeted attacks. Future directions are applying our framework to other random-search based attacks and threat models as well as learning controllers for sampling positions or even geometric primitives (going beyond squares).

Ethical and Societal Impact This work contributes to the field of black-box adversarial attacks, which can be used for benign purposes like reliably evaluating the robustness of ML systems as well as malign ones such as identifying and exploiting weaknesses of these systems. Increasing the query-efficiency and success rate of black-box attacks can amplify safety and security concerns in domains such as highly automated driving or robotics. Meta Square Attack allows more efficient generation of imperceptible image distortions that may allow bypassing automated content-control systems for filtering images with violent, pornographic, or otherwise offensive content. We are optimistic that the research on adversarial attacks contributes to developing defenses and mitigation strategies that outweigh these risks in the medium term. A general mitigation strategy could be to add a check to a system which rejects predictions for a sequence of inputs which all differ by at most an ℓ_p distance of some ϵ . This would make most score-based black-box attacks for image-specific perturbations ineffective, including Meta Square Attack.

Acknowledgements

Matthias Hein is a member of the Machine Learning Cluster of Excellence, EXC number 2064/1 – Project number 390727645 and of the BMBF Tübingen AI Center, FKZ: 01IS18039B.

References

- [1] Maksym Andriushchenko, Francesco Croce, Nicolas Flammarion, and Matthias Hein. Square attack: a query-efficient black-box adversarial attack via random search. In *ECCV*, 2020.
- [2] Francesco Croce and Matthias Hein. Reliable evaluation of adversarial robustness with an ensemble of diverse parameter-free attacks. In *ICML*, 2020.
- [3] Gavin Weiguang Ding, Yash Sharma, Kry Yik Chau Lui, and Ruitong Huang. MMA training: Direct input space margin maximization through adversarial training. In *ICLR*, 2020.
- [4] C. Szegedy, W. Zaremba, I. Sutskever, J. Bruna, D. Erhan, I. Goodfellow, and R. Fergus. Intriguing properties of neural networks. In *ICLR*, 2014.
- [5] Anurag Ranjan, Joel Janai, Andreas Geiger, and Michael J. Black. Attacking optical flow. In *ICCV*, 2019.
- [6] Andrew Ilyas, Shibani Santurkar, Dimitris Tsipras, Logan Engstrom, Brandon Tran, and Aleksander Madry. Adversarial examples are not bugs, they are features. In *NeurIPS*, 2019.
- [7] G. Katz, C. Barrett, D. Dill, K. Julian, and M. Kochenderfer. Reluplex: An efficient smt solver for verifying deep neural networks. In *CAV*, 2017.
- [8] Nicholas Carlini and David A. Wagner. Towards evaluating the robustness of neural networks. *IEEE Symposium on Security and Privacy (SP)*, pages 39–57, 2017.
- [9] Ian J. Goodfellow, Jonathon Shlens, and Christian Szegedy. Explaining and harnessing adversarial examples. In *ICLR*, 2015.
- [10] Anirban Chakraborty, M. Alam, Vishal Dey, A. Chattopadhyay, and Debdeep Mukhopadhyay. Adversarial attacks and defences: A survey. *arXiv: 1810.00069*, 2018.
- [11] A. Athalye, N. Carlini, and D. Wagner. Obfuscated gradients give a false sense of security: Circumventing defenses to adversarial examples. In *ICML*, 2018.
- [12] A. Al-Dujaili and U.-M. O’Reilly. There are no bit parts for sign bits in black-box attacks. In *ICLR*, 2020.
- [13] J. Chen, M. I Jordan, and Wainwright M. J. HopSkipJumpAttack: a query-efficient decision-based attack. In *IEEE Symposium on Security and Privacy (SP)*, 2019.
- [14] S. N. Shukla, A. K. Sahu, D. Willmott, and Z. Kolter. Black-box adversarial attacks with Bayesian optimization. *arXiv preprint arXiv:1909.13857*, 2019.
- [15] A. Ilyas, L. Engstrom, A. Athalye, and J. Lin. Black-box adversarial attacks with limited queries and information. *ICML*, 2018.
- [16] Z. Yan, Y. Guo, and C. Zhang. Subspace attack: Exploiting promising subspaces for query-efficient black-box attacks. In *NeurIPS*, 2019.
- [17] S. Cheng, Y. Dong, T. Pang, H. Su, and J. Zhu. Improving black-box adversarial attacks with a transfer-based prior. In *NeurIPS*, 2019.
- [18] M. Seungyong, A. Gaon, and O. S. Hyun. Parsimonious black-box adversarial attacks via efficient combinatorial optimization. In *ICML*, 2019.
- [19] M. Alzantot, Y. Sharma, S. Chakraborty, and M. Srivastava. Genattack: practical black-box attacks with gradient-free optimization. *Genetic and Evolutionary Computation Conference (GECCO)*, 2019.

- [20] Huichen Li, Xiaojun Xu, Xiaolu Zhang, Shuang Yang, and Bo Li. Qeba: Query-efficient boundary-based blackbox attack. In *CVPR*, 2020.
- [21] Zhichao Huang, Yaowei Huang, and Tong Zhang. Corrattack: Black-box adversarial attack with structured search. *arXiv:2010.01250*, 2020.
- [22] Florian Tramer, Nicholas Carlini, Wieland Brendel, and Aleksander Madry. On adaptive attacks to adversarial example defenses. In *NeurIPS*, 2020.
- [23] C. Guo, J. R Gardner, Y. You, A. G. Wilson, and K. Q. Weinberger. Simple black-box adversarial attacks. In *ICML*, 2019.
- [24] Francesco Croce, Maksym Andriushchenko, Naman D. Singh, Nicolas Flammarion, and Matthias Hein. Sparse-rs: a versatile framework for query-efficient sparse black-box adversarial attacks. *arXiv:2006.12834*, 2020.
- [25] Francesco Croce and Matthias Hein. Mind the box: l_1 -apgd for sparse adversarial attacks on image classifiers. In *ICML*, 2021.
- [26] A. Madry, A. Makelov, L. Schmidt, D. Tsipras, and A. Valdu. Towards deep learning models resistant to adversarial attacks. In *ICLR*, 2018.
- [27] Kaiming He, X. Zhang, Shaoqing Ren, and Jian Sun. Deep residual learning for image recognition. In *CVPR*, 2016.
- [28] Francesco Croce, Maksym Andriushchenko, Vikash Sehwal, Nicolas Flammarion, Mung Chiang, Prateek Mittal, and Matthias Hein. Robustbench: a standardized adversarial robustness benchmark. *arXiv:2010.09670*, 2020.
- [29] Zhichao Huang and Tong Zhang. Black-box adversarial attack with transferable model-based embedding. In *ICLR*, 2020.
- [30] Wieland Brendel, Jonas Rauber, and Matthias Bethge. Decision-based adversarial attacks: Reliable attacks against black-box machine learning models. In *ICLR*, 2018.
- [31] J. Uesato, B. O’Donoghue, A. Van den Oord, and P. Kohli. Adversarial risk and the dangers of evaluating against weak attacks. In *ICML*, 2018.
- [32] A. N. Bhagoji, W. He, B. Li, and D. Song. Practical black-box attacks on deep neural networks using efficient query mechanisms. In *ECCV*, 2018.
- [33] L. Meunier, J. Atif, and O. Teytaud. Yet another but more efficient black-box adversarial attack: tiling and evolution strategies. *arXiv preprint, arXiv:1910.02244*, 2019.
- [34] Timothy Hospedales, Antreas Antoniou, Paul Micaelli, and Amos Storkey. Meta-learning in neural networks: A survey. *IEEE PAMI*, 2021.
- [35] Tianlong Chen, Xiaohan Chen, Wuyang Chen, Howard Heaton, Jialin Liu, Zhangyang Wang, and Wotao Yin. Learning to optimize: A primer and a benchmark. *arXiv: 2103.12828*, 2021.
- [36] Marcin Andrychowicz, Misha Denil, Sergio Gomez Colmenarejo, Matthew W. Hoffman, D. Pfau, Tom Schaul, and N. D. Freitas. Learning to learn by gradient descent by gradient descent. In *NIPS*, 2016.
- [37] Yutian Chen, Matthew W. Hoffman, Sergio Gomez Colmenarejo, Misha Denil, Timothy P. Lillicrap, Matt Botvinick, and Nando de Freitas. Learning to learn without gradient descent by gradient descent. In *ICML*, 2017.
- [38] Yuanhao Xiong and Cho-Jui Hsieh. Improved adversarial training via learned optimizer. In *ECCV*, 2020.
- [39] Yangjun Ruan, Yuanhao Xiong, Sashank Reddi, Sanjiv Kumar, and Cho-Jui Hsieh. Learning to learn by zeroth-order oracle. In *ICLR*, 2020.

- [40] Chelsea Finn, Pieter Abbeel, and Sergey Levine. Model-agnostic meta-learning for fast adaptation of deep networks. In *ICML*, 2017.
- [41] Alex Nichol, Joshua Achiam, and John Schulman. On first-order meta-learning algorithms. *arXiv:1803.02999*, 2018.
- [42] Jiawei Du, Hu Zhang, Joey Tianyi Zhou, Yi Yang, and Jiashi Feng. Query-efficient meta attack to deep neural networks. In *ICLR*, 2020.
- [43] Chengyuan Yao, Pavol Bielik, Petar Tsankov, and Martin Vechev. Automated discovery of adaptive attacks on adversarial defenses. *arXiv:2102.11860*, 2021.
- [44] Jan Hendrik Metzen, Nicole Finnie, and Robin Huttmacher. Meta adversarial training against universal patches. *arXiv:2101.11453*, 2021.
- [45] D Yin, R. G. Lopes, J. Shlens, E. D Cubuk, and J. Gilmer. A Fourier perspective on model robustness in computer vision. In *NeurIPS*, 2019.
- [46] Eric Jang, Shixiang Gu, and Ben Poole. Categorical reparametrization with gumbel-softmax. In *ICLR*, 2017.
- [47] Chris J. Maddison, Andriy Mnih, and Yee Whye Teh. The Concrete Distribution: A Continuous Relaxation of Discrete Random Variables. In *ICLR*, 2017.
- [48] Alex Krizhevsky and Geoffrey Hinton. Learning multiple layers of features from tiny images. Technical report, University of Toronto, 2009.
- [49] Gavin Weiguang Ding, Luyu Wang, and Xiaomeng Jin. AdverTorch v0.1: An adversarial robustness toolbox based on pytorch. *arXiv:1902.07623*, 2019.
- [50] Ilya Loshchilov and Frank Hutter. SGDR: stochastic gradient descent with warm restarts. In *ICLR*, 2017.
- [51] Eric Wong, Leslie Rice, and J. Zico Kolter. Fast is better than free: Revisiting adversarial training. In *ICLR*, 2020.
- [52] Lang Huang, Chao Zhang, and Hongyang Zhang. Self-adaptive training: beyond empirical risk minimization. In *NeurIPS*, 2020.
- [53] Dongxian Wu, Shu tao Xia, and Yisen Wang. Adversarial weight perturbation helps robust generalization. In *NeurIPS*, 2020.
- [54] Jiequan Cui, Shu Liu, Liwei Wang, and Jiaya Jia. Learnable boundary guided adversarial training. In *ICCV*, 2021.
- [55] Hadi Salman, Andrew Ilyas, Logan Engstrom, Ashish Kapoor, and Aleksander Madry. Do adversarially robust imagenet models transfer better? In *NeurIPS*, 2020.
- [56] Logan Engstrom, Andrew Ilyas, Hadi Salman, Shibani Santurkar, and Dimitris Tsipras. Robustness (python library), 2019. URL <https://github.com/MadryLab/robustness>.
- [57] Jia Deng, Wei Dong, Richard Socher, Li-Jia Li, Kai Li, and Li Fei-Fei. Imagenet: A large-scale hierarchical image database. In *2009 IEEE conference on computer vision and pattern recognition*, pages 248–255. Ieee, 2009.
- [58] Kaiming He, Xiangyu Zhang, Shaoqing Ren, and Jian Sun. Deep residual learning for image recognition. In *CVPR*, 2016.
- [59] Karen Simonyan and Andrew Zisserman. Very deep convolutional networks for large-scale image recognition. In *ICLR*, 2015.
- [60] Christian Szegedy, Vincent Vanhoucke, Sergey Ioffe, Jonathon Shlens, and Zbigniew Wojna. Rethinking the inception architecture for computer vision. In *CVPR*, 2016.
- [61] Leslie Rice, Eric Wong, and J. Zico Kolter. Overfitting in adversarially robust deep learning. In *ICML*, 2020.

- [62] Sven Gowal, Chongli Qin, Jonathan Uesato, Timothy Mann, and Pushmeet Kohli. Uncovering the limits of adversarial training against norm-bounded adversarial examples. *arXiv:2010.03593*, 2021.
- [63] Yair Carmon, Aditi Raghunathan, Ludwig Schmidt, Percy Liang, and John C. Duchi. Unlabeled data improves adversarial robustness. In *NeurIPS*, 2019.
- [64] Maksym Andriushchenko and Nicolas Flammarion. Understanding and improving fast adversarial training. In *NeurIPS*, 2020.
- [65] Hongyang Zhang, Yaodong Yu, Jiantao Jiao, Eric P. Xing, Laurent El Ghaoui, and Michael I. Jordan. Theoretically principled trade-off between robustness and accuracy. In *ICML*, 2019.
- [66] Dan Hendrycks, Kimin Lee, and Mantas Mazeika. Using pre-training can improve model robustness and uncertainty. In *ICML*, 2019.
- [67] Yisen Wang, Difan Zou, Jinfeng Yi, James Bailey, Xingjun Ma, and Quanquan Gu. Improving adversarial robustness requires revisiting misclassified examples. In *ICLR*, 2020.
- [68] Chawin Sitawarin, Supriyo Chakraborty, and David Wagner. Improving adversarial robustness through progressive hardening. *arXiv:2003.09347*, 2020.
- [69] Jingfeng Zhang, Jianing Zhu, Gang Niu, Bo Han, Masashi Sugiyama, and Mohan Kankanhalli. Geometry-aware instance-reweighted adversarial training. In *ICLR*, 2021.
- [70] Jingfeng Zhang, Xilie Xu, Bo Han, Gang Niu, Lizhen Cui, Masashi Sugiyama, and Mohan Kankanhalli. Attacks which do not kill training make adversarial learning stronger. In *ICML*, 2020.
- [71] Dinghui Zhang, Tianyuan Zhang, Yiping Lu, Zhanxing Zhu, and Bin Dong. You only propagate once: Accelerating adversarial training via maximal principle. In *NeurIPS*, 2019.
- [72] Maximilian Augustin, Alexander Meinke, and Matthias Hein. Adversarial robustness on in- and out-distribution improves explainability. In *ECCV*, 2020.
- [73] Jérôme Rony, Luiz G. Hafemann, Luiz S. Oliveira, Ismail Ben Ayed, Robert Sabourin, and Eric Granger. Decoupling direction and norm for efficient gradient-based l2 adversarial attacks and defenses. In *CVPR*, 2019.
- [74] Adam Paszke, Sam Gross, Francisco Massa, Adam Lerer, James Bradbury, Gregory Chanan, Trevor Killeen, Zeming Lin, Natalia Gimelshein, Luca Antiga, Alban Desmaison, Andreas Köpf, Edward Yang, Zach DeVito, Martin Raison, Alykhan Tejani, Sasank Chilamkurthy, Benoit Steiner, Lu Fang, Junjie Bai, and Soumith Chintala. Pytorch: An imperative style, high-performance deep learning library. In *NeurIPS*, 2019.

A Appendix

A.1 Full experimental results

In this section we provide the full experimental results that extend the results demonstrated in the Section 4.2. Table 8 demonstrates the evaluation on 16 robustly trained CIFAR10 models from RobustBench [28] that was summarized in the Table 2. We consider four configurations of the attack for each of the models. SA and AA correspond to the update size schedules proposed by Andriushchenko et al. [1] and Croce and Hein [2] respectively. "Uni" denotes sampling the color for the update uniformly. MSA_s+MSA_c is a combination of an update size controller with the color sampling controller that we denoted as MSA in the Section 4.2. MSA_s+Uni is an ablated version in which we only use an update size controller MSA_s . The clean and robust accuracy of the models are taken from <https://robustbench.github.io/>.

Table 8: We compare the update size controller MSA_s to the schedules from the SA [1] and the AA [2] in the ℓ_∞ threat model with $\epsilon = 8/255$ on 1000 CIFAR10 test images. We also compare the uniform color sampling denoted as "Uni" to our color controller MSA_c . Averaged across at least 3 runs with different random seeds.

Model	Accuracy (%)		Square size	Color	Query budget			
	Clean	Robust			500	1000	2500	5000
Wong et al. [51]	83.34	43.21	SA	Uni	69.7±0.15	63.5±0.10	55.1±0.04	50.8±0.08
			AA	Uni	69.5±0.21	63.9±0.10	57.4±0.07	53.6±0.06
			MSA_s	Uni	63.9±0.11	59.8±0.10	54.0±0.16	51.1±0.08
			MSA_s	MSA_c	63.9±0.12	59.1±0.09	53.0±0.16	49.8±0.08
Ding et al. [3]	84.36	41.44	SA	Uni	68.7±0.20	63.2±0.28	57.8±0.13	54.9±0.17
			AA	Uni	66.6±0.18	62.2±0.14	57.5±0.12	55.0±0.20
			MSA_s	Uni	62.4±0.15	59.4±0.09	56.1±0.10	54.6±0.06
			MSA_s	MSA_c	62.2±0.14	59.1±0.16	55.9±0.15	54.1±0.15
Engstrom et al. [56]	87.03	49.25	SA	Uni	72.8±0.19	67.4±0.21	59.9±0.17	56.3±0.07
			AA	Uni	71.9±0.1	67.9±0.14	61.6±0.12	58.0±0.06
			MSA_s	Uni	67.9±0.12	64.2±0.15	58.9±0.05	56.4±0.12
			MSA_s	MSA_c	67.8±0.12	63.4±0.18	58.2±0.06	55.9±0.04
Gowal et al. [62]	89.48	62.76	SA	Uni	80.6±0.09	76.7±0.06	70.8±0.14	67.5±0.07
			AA	Uni	80.0±0.17	76.8±0.11	72.2±0.10	69.2±0.08
			MSA_s	Uni	76.9±0.05	73.7±0.05	69.8±0.13	67.6±0.04
			MSA_s	MSA_c	76.9±0.07	73.4±0.13	69.0±0.08	67.2±0.04
Carmon et al. [63]	89.69	59.53	SA	Uni	79.0±0.15	76.0±0.14	68.2±0.07	65.4±0.09
			AA	Uni	78.0±0.10	74.5±0.11	69.6±0.04	67.1±0.05
			MSA_s	Uni	74.4±0.09	70.8±0.06	67.5±0.07	65.6±0.07
			MSA_s	MSA_c	74.6±0.10	70.3±0.07	67.0±0.07	65.4±0.08
Huang et al. [52]	83.48	53.34	SA	Uni	72.3±0.1	66.6±0.16	60.5±0.09	57.3±0.08
			AA	Uni	70.6±0.10	66.5±0.07	61.2±0.10	58.5±0.11
			MSA_s	Uni	66.4±0.12	63.4±0.08	59.2±0.07	57.4±0.15
			MSA_s	MSA_c	66.1±0.10	62.9±0.15	58.7±0.05	56.8±0.08
Andriushchenko and Flammarion [64]	79.84	43.93	SA	Uni	66.0±0.22	60.5±0.24	54.0±0.06	50.2±0.03
			AA	Uni	64.6±0.12	60.2±0.22	55.7±0.10	52.1±0.15
			MSA_s	Uni	60.4±0.09	57.0±0.07	52.5±0.19	50.0±0.06
			MSA_s	MSA_c	60.1±0.07	56.8±0.15	51.9±0.15	49.4±0.22
Zhang et al. [65]	84.92	53.08	SA	Uni	72.3±0.03	67.2±0.19	62.0±0.09	59.0±0.06
			AA	Uni	70.8±0.22	67.2±0.17	62.7±0.10	60.3±0.17
			MSA_s	Uni	67.5±0.06	64.2±0.18	60.8±0.07	59.0±0.07
			MSA_s	MSA_c	66.8±0.09	63.9±0.07	60.4±0.06	58.7±0.13
Hendrycks et al. [66]	87.11	54.92	SA	Uni	75.3±0.30	69.8±0.19	64.2±0.15	60.8±0.00
			AA	Uni	74.7±0.17	70.5±0.26	64.7±0.12	62.8±0.15
			MSA_s	Uni	71.1±0.07	66.6±0.15	63.2±0.12	61.0±0.07
			MSA_s	MSA_c	70.6±0.17	66.1±0.12	62.7±0.13	60.4±0.15
Wang et al. [67]	87.50	56.29	SA	Uni	77.7±0.12	72.2±0.03	65.8±0.15	62.2±0.03
			AA	Uni	76.7±0.06	72.8±0.12	67.6±0.20	64.0±0.17
			MSA_s	Uni	73.1±0.18	69.8±0.09	64.9±0.15	62.3±0.03
			MSA_s	MSA_c	72.7±0.07	69.5±0.09	64.3±0.18	62.0±0.07
Cui et al. [54]	88.22	52.86	SA	Uni	75.5±0.22	69.6±0.09	62.9±0.20	59.2±0.15
			AA	Uni	74.2±0.13	70.2±0.07	64.8±0.07	61.1±0.23
			MSA_s	Uni	70.1±0.07	66.7±0.18	61.8±0.12	59.7±0.03
			MSA_s	MSA_c	70.0±0.15	66.2±0.25	60.8±0.09	59.0±0.06

Model	Accuracy (%)		Square size	Color	Query budget			
	Clean	Robust			500	1000	2500	5000
Sitawarin et al. [68]	86.84	50.72	SA	Uni	73.4±0.06	66.4±0.10	61.1±0.07	57.4±0.12
			AA	Uni	72.0±0.20	66.8±0.23	62.3±0.20	59.4±0.12
			MSA _s	Uni	66.7±0.06	63.6±0.03	60.3±0.17	57.5±0.03
			MSA _s	MSA _c	66.9±0.00	63.1±0.09	59.3±0.12	57.0±0.00
Wu et al. [53]	85.36	56.17	SA	Uni	75.0±0.19	69.7±0.21	63.8±0.12	60.4±0.07
			AA	Uni	73.6±0.03	69.5±0.25	64.5±0.07	62.3±0.07
			MSA _s	Uni	69.6±0.09	66.1±0.20	63.1±0.17	60.7±0.07
			MSA _s	MSA _c	69.4±0.23	65.7±0.12	62.6±0.12	60.3±0.03
Zhang et al. [69]	89.36	59.64	SA	Uni	79.6±0.27	74.6±0.03	66.9±0.07	64.0±0.07
			AA	Uni	78.4±0.06	75.3±0.03	68.9±0.06	65.6±0.03
			MSA _s	Uni	75.1±0.09	71.4±0.09	66.2±0.20	64.3±0.06
			MSA _s	MSA _c	75.0±0.19	70.4±0.17	65.6±0.09	63.8±0.10
Zhang et al. [70]	84.52	53.51	SA	Uni	73.4±0.03	67.5±0.09	61.5±0.12	58.9±0.09
			AA	Uni	72.3±0.06	67.7±0.00	62.3±0.06	60.4±0.06
			MSA _s	Uni	67.4±0.09	63.6±0.25	61.2±0.03	59.3±0.10
			MSA _s	MSA _c	67.6±0.06	63.5±0.09	60.6±0.10	59.0±0.10
Zhang et al. [71]	87.20	44.83	SA	Uni	73.1±0.00	66.2±0.26	56.5±0.15	52.5±0.12
			AA	Uni	71.8±0.23	66.5±0.07	59.2±0.09	54.7±0.12
			MSA _s	Uni	66.9±0.18	61.9±0.09	55.2±0.15	52.6±0.09
			MSA _s	MSA _c	66.4±0.06	60.8±0.15	54.6±0.09	51.9±0.12

Table 9 provides an extended version of the Table 4 in which we additionally provide the results for the ablated version MSA_s+Uni to demonstrate that the update size controller on its own provides better results than the considered baselines SA [1] and AA [2]. However, if we add a color sampling controller MSA_c, we manage to further improve the robust accuracy estimate.

Table 10 demonstrates the the results for the ℓ_2 threat model for five ℓ_2 robust models from Robust-Bench [28]. We have chosen the models for which Croce and Hein [2] provide their evaluation of the Square Attack. They evaluate on the whole CIFAR10 test set and we evaluate on a subset of 1000 test images. Therefore their estimate is not identical to our entry AA+Uni. But we still provide it as Sq AA [2] in the Table 10 for additional reference.

A.2 Meta-training the Controllers

The meta-training of controllers was described in Section 3 and Section 4.1. We summarize it schematically for the case of general random-search based black-box attack (Figure 3) and for the Meta Square Attack (Figure 4). We provide some additional details and illustrate the learning curves.

Table 9: Results of attacking 1000 ImageNet validation set images with ℓ_∞ threat model and $\epsilon = 4/255$ as in Croce and Hein [2]. For the SA update size schedule, we use the parameter $p^0 = 0.05$ as suggested in Andriushchenko et al. [1]. AA and Uni are defined as in Table 1. MSA_s and MSA_c are meta-trained on CIFAR10 (see Section 4.1 for details). We report mean and standard error of robust accuracy for different queries budgets across 3 runs with different random seeds.

Model	Accuracy (%)		Square size	Color	Query budget			
	Clean	Robust			500	1000	2500	5000
resnet18 Salman et al. [55]	52.5	25.0	SA	Uni	50.6±1.43	48.1±1.18	43.9±1.00	40.3±1.21
			AA	Uni	45.2±1.09	43.5±0.86	41.0±1.07	39.0±1.21
			MSA _s	Uni	43.4±0.94	41.7±1.13	39.5±1.07	38.3±1.33
			MSA _s	MSA _c	43.3±1.00	41.7±0.94	39.1±1.23	37.8±1.36
resnet50 Engstrom et al. [56]	63.4	27.6	SA	Uni	59.8±0.64	57.2±0.79	52.9±1.11	48.6±1.31
			AA	Uni	54.6±0.99	52.8±1.09	50.3±1.43	48.1±1.18
			MSA _s	Uni	52.6±1.07	51.2±1.40	48.3±1.22	45.8±1.26
			MSA _s	MSA _c	52.5±1.23	50.8±1.47	48.0±1.15	45.8±1.35

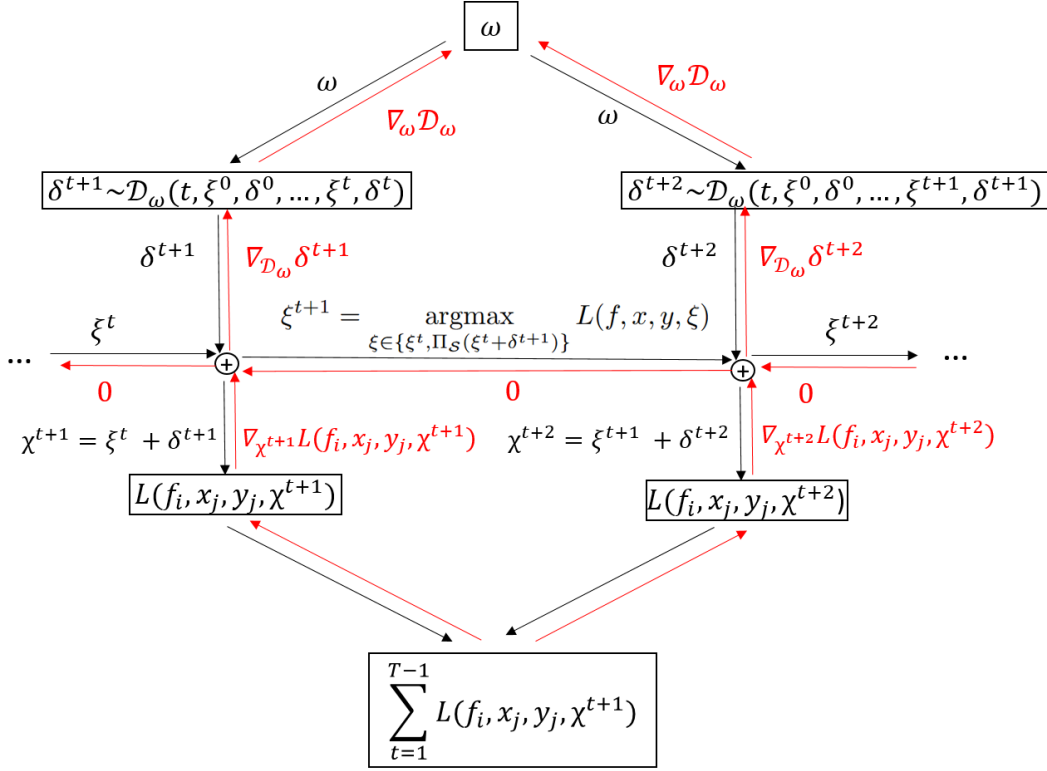


Figure 3: Schematic illustration of the general meta-learning procedure described in Section 3.2 for two subsequent steps of the random search attack (3). We describe forward (black) and backward (red) pass. $\nabla_x f$ denotes gradient for scalar-valued functions f and Jacobian for vector-valued functions. Differential expressions with search distribution \mathcal{D}_ω are informal and in need to be handled with reparametrization trick or other methods when applying the method to particular attacks (for examples see Section 3.3). Please note that the gradient with respect to ξ^t is set to 0 for all t (see Section 3.2).

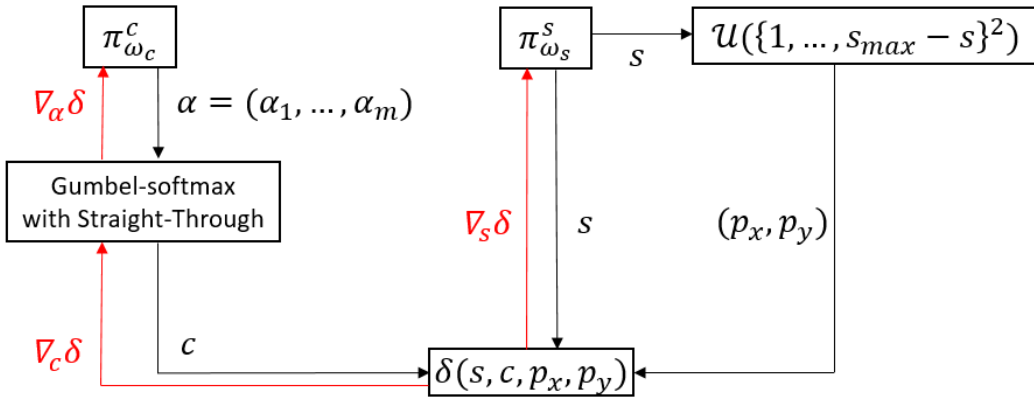


Figure 4: Illustration of Meta Square Attack described in Section 3.3. The search distribution $\mathcal{D}_{(s,c)}$ depends on parameters s and α that are provided by the update size controller $\pi_{\omega_c}^c$ and the color controller $\pi_{\omega_s}^s$, respectively. Square positions (p_x, p_y) are sampled from the uniform distribution $\mathcal{U}(\{1, \dots, s_{max} - s\}^2)$

Table 10: MSA_s^2 is the update size controller trained for the ℓ_2 attack on a CIFAR10 model described in the Section 4.1. MSA_s^∞ denotes the update size controller meta-trained for the ℓ_∞ Square Attack on CIFAR10. The color controller MSA_c is the same as for the ℓ_∞ case. We compare to the ℓ_2 versions of SA [1] and AA [2] with $\epsilon = 0.5$ on 1000 CIFAR10 images.

Model	Accuracy (%)			Square size	Color	Query budget			
	Clean	Robust	Sq AA [2]			500	1000	2500	5000
Ding et al. [3]	88.02	66.09	76.99	SA	Uni	85.5±0.06	83.9±0.08	81.1±0.00	78.7±0.06
				AA	Uni	82.8±0.09	81.4±0.06	79.2±0.00	77.7±0.15
				MSA_s^∞	Uni	82.6±0.09	81.7±0.12	79.8±0.12	77.9±0.07
				MSA_s^∞	MSA_c	82.5±0.22	81.5±0.03	78.5±0.06	76.9±0.17
				AA	MSA_c	82.6±0.03	81.1±0.17	78.2±0.10	76.5±0.09
				MSA_s^2	MSA_c	82.3±0.03	80.9±0.07	77.4±0.09	75.8±0.19
Rice et al. [61]	88.67	67.68	79.01	SA	Uni	86.3±0.07	84.7±0.10	81.4±0.15	79.7±0.07
				AA	Uni	83.7±0.12	81.4±0.09	79.9±0.09	78.6±0.18
				MSA_s^∞	Uni	83.2±0.12	81.8±0.07	80.1±0.07	79.1±0.09
				MSA_s^∞	MSA_c	83.0±0.15	81.2±0.06	79.6±0.03	78.3±0.03
				AA	MSA_c	83.4±0.12	81.2±0.10	79.3±0.09	78.0±0.06
				MSA_s^2	MSA_c	82.6±0.09	81.0±0.07	78.7±0.03	76.9±0.25
Augustin et al. [72]	91.08	72.91	83.10	SA	Uni	89.0	88.4	86.9	84.2
				AA	Uni	87.8±0.03	86.8±0.09	84.8±0.17	83.3±0.17
				MSA_s^∞	Uni	87.7±0.06	87.0±0.09	85.2±0.03	83.4±0.10
				MSA_s^∞	MSA_c	87.4±0.15	86.5±0.12	84.1±0.20	82.8±0.13
				AA	MSA_c	87.7±0.12	86.6±0.09	83.9±0.13	82.7±0.09
				MSA_s^2	MSA_c	87.5±0.12	86.3±0.06	83.4±0.03	81.8±0.07
Engstrom et al. [56]	90.83	69.24	80.92	SA	Uni	87.3	86.1	84.0	80.8
				AA	Uni	85.3±0.06	83.7±0.15	81.5±0.24	79.5±0.18
				MSA_s^∞	Uni	85.2±0.12	84.2±0.17	82.0±0.09	79.9±0.07
				MSA_s^∞	MSA_c	85.1±0.07	83.7±0.03	80.6±0.06	78.8±0.09
				AA	MSA_c	85.2±0.07	83.5±0.07	80.6±0.06	78.5±0.15
				MSA_s^2	MSA_c	84.7±0.09	83.1±0.06	79.7±0.13	77.4±0.00
Rony et al. [73]	89.05	66.44	78.05	SA	Uni	85.4	83.5	80.5	78.3
				AA	Uni	82.0±0.10	80.8±0.10	78.9±0.03	77.0±0.15
				MSA_s^∞	Uni	81.8±0.03	81.0±0.10	79.1±0.15	77.7±0.07
				MSA_s^∞	MSA_c	81.9±0.07	80.7±0.06	78.5±0.17	76.5±0.03
				AA	MSA_c	81.9±0.09	80.6±0.12	78.3±0.07	76.2±0.03
				MSA_s^2	MSA_c	81.6±0.03	80.4±0.00	77.2±0.00	75.7±0.09

As discussed in Section 3.3, we maximize the following meta-objective:

$$R(F, D, \omega) = \frac{1}{T} \sum_{f_i} \sum_{(x_j, y_j)} \sum_{t=1}^{T-1} L(f_i, x_j, y_j, \Pi_S(\xi^t + \delta^{t+1})), \quad (6)$$

where $\delta^{t+1} \sim \mathcal{D}_\omega(t, \xi^0, \delta^0, \dots, \xi^t, \delta^t)$. Recall from Section 3.1 that $L(f, x, y, \xi) := l(f(a(x, \xi)), y)$. As discussed in Section 3.3, we use total loss improvement over attack as our meta-loss. Therefore, we choose l in a way that it represents loss improvement caused by the update ξ i. e.

$$l(f(a(x, \xi)), y) = (h(f(a(x, \xi)), y) - h_{max})_+, \quad (7)$$

where $(x)_+$ is positive part function, $h(p, q)$ is cross-entropy loss and h_{max} is the largest cross-entropy value obtained so far. In our case at step t we have $h_{max} = h(f(a(x, \Pi_S(\xi^t)), y)$ by design of the random search attack (3). Finally, instead of solving the problem of maximizing $R(F, D, \omega)$, we are solving the equivalent problem of minimizing $-R(F, D, \omega)$. Therefore, the loss that we use for training our controllers for Meta Square Attack is:

$$R_{MSA}(F, D, \omega) = -\frac{1}{T} \sum_{f_i} \sum_{(x_j, y_j)} \sum_{t=1}^{T-1} (h(f_i(a(x_j, \Pi_S(\xi^t + \delta^{t+1}))), y_j) - h(f_i(a(x_j, \Pi_S(\xi^t))), y_j))_+. \quad (8)$$

As discussed in Section 4, we use 1000 CIFAR10 test set images for meta-training and different 1000 images for evaluation. We use the default order of CIFAR10 images (i. e., we do not shuffle).

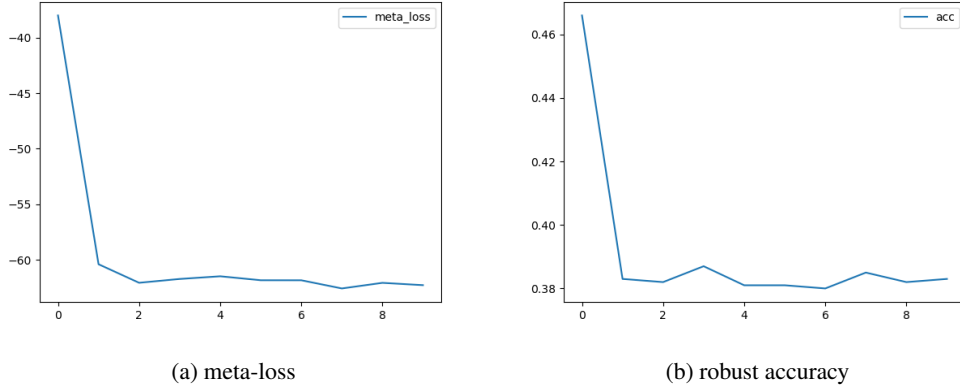


Figure 5: Meta-loss and robust accuracy on the training set during meta-training.

For meta-training we use images from 0 to 999 and for evaluation we use images from 9000 to 9999. Figure 5 demonstrates the minimization of $R_{MSA}(F, D, \omega)$ and corresponding behavior of the accuracy on the training set. One can see that the proposed meta-loss $R_{MSA}(F, D, \omega)$ serves as a reasonable differentiable proxy for the robust accuracy. We observe that the loss reaches a close-to-minimal value already after two epochs.

A.3 Square relaxation

In Section 3.3, we formalize update size and color controllers that we learn for Meta Square Attack. Here we provide additional details on how we avoid blocking of gradient flow in our optimization scheme using relaxed square sampling.

$$g = \frac{1}{T} \sum_{f_i} \sum_{(x_j, y_j)} \sum_{t=1}^{T-1} \nabla_{\omega} L(f_i, x_j, y_j, \xi^t + \delta^{t+1}), \quad (9)$$

for simplicity assuming that projection operator Π_S in Equation (5) is incorporated into L . Since we rewrite $\nabla_{\omega} L(f_i, x_j, y_j, \xi^t + \delta^{t+1}) = \nabla_{\delta^{t+1}} L(f_i, x_j, y_j, \xi^t + \delta^{t+1}) \nabla_{\omega} \delta^{t+1}$, we need to compute the Jacobian $\nabla_{\omega} \delta^{t+1}$ of update vector δ^{t+1} with respect to meta-parameters ω .

Recall that in Section 3.3 we denote $\omega = (\omega_s, \omega_c)$ and consider controllers $\pi_{\omega_s}^s$ and $\pi_{\omega_c}^c$ for the update size and color respectively. Since computing $\nabla_{\omega_c} \delta^{t+1}$ is done via Gumbel softmax [46, 47], here we concentrate on computing $\nabla_{\omega_s} \delta^{t+1}$. Since $\pi_{\omega_s}^s$ only controls update size, we assume its position and color to be fixed when computing the gradient.

In SA [1] each update is parametrized by an integer square width from $\{1, \dots, w\}$ where w is image width. This parameter is obtained by rounding real value s obtained from the update size schedule to the closest integer in the feasible range. During meta-training we cannot round the output s of $\pi_{\omega_s}^s$ since in that case we get $\nabla_{\omega_s} \delta^{t+1} = 0$ almost everywhere. Therefore, we propose a differentiable relaxation (see Figure 6). The inner part of the square with width $odd(s) = 2 \cdot \lfloor \frac{s-1}{2} \rfloor + 1$ is filled with the sampled color c completely. The color of pixels in the 1-pixel boundary is interpolated between the background color c_0 and the new color c as: $k \cdot c + (1 - k) \cdot c_0$. The coefficient k of the new color is equal to the fraction that the square of non-integer width s would occupy in the respective pixel. Therefore, for the 4-neighborhood the new color fraction is $k = \frac{s - odd(s)}{2}$ and for the pixel of 8-neighborhood that do not belong to 4-neighborhood $k = (\frac{s - odd(s)}{2})^2$.

A.4 Additional analysis of the learned controllers

In this Section we provide some additional analysis of the meta-learned controllers that we have started in the Section 4.3.

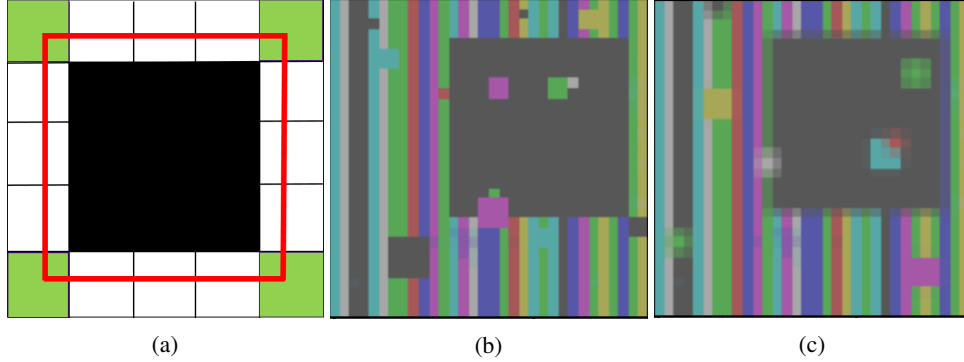


Figure 6: (a) illustration of a square with non-integer size s (red), size $odd(s)$ (black), 4-neighborhood (white) and 8-neighborhood pixels that do not belong to 4-neighborhood (green), (b) standard square attack perturbation, (c) square attack perturbation with proposed square relaxation.

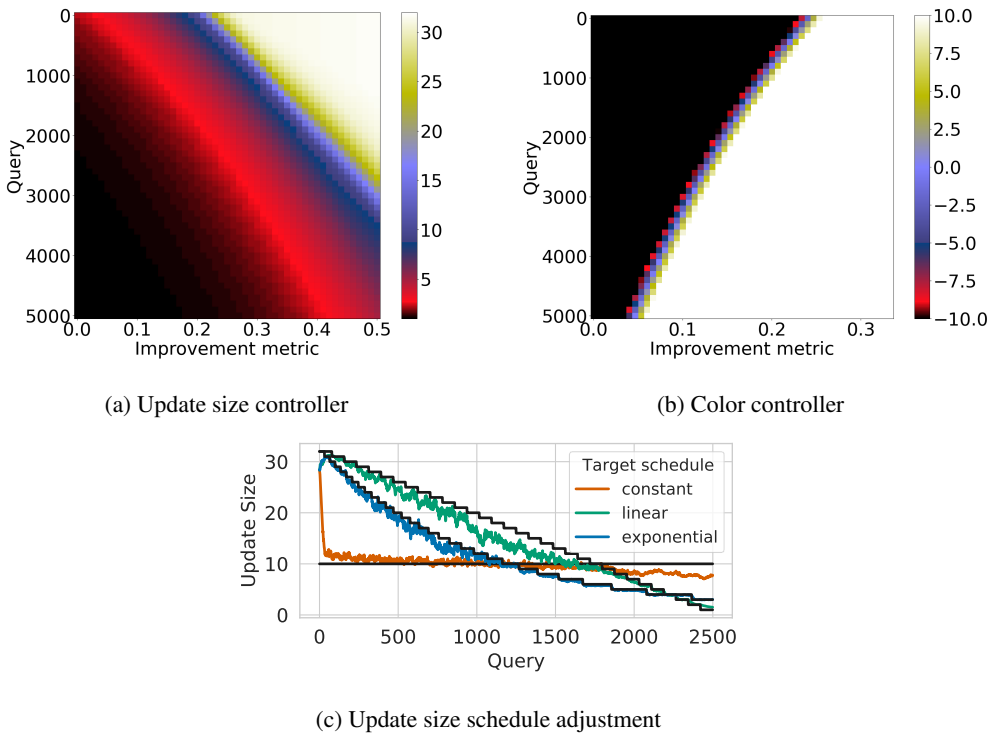


Figure 7: Additional analysis of the meta-learned controllers. The plot of the (a) update size controller MSA_s and (b) color controller MSA_c as functions of their inputs. (c) MSA_s adjustment to the target schedules (averaged over 25 runs).

Since our controllers are functions of 2 inputs as described in the Section 3.3 we can illustrate the dependence of their outputs on these inputs. We show it in Figure 7a for the update size controller and Figure 7b for the color controller.

The Figure 7c illustrates observed schedules for idealized (and untypical) target schedules: these target schedules are unknown to the controller and are encoded in the success probabilities by setting $p(r^t = 1) = 0.4$ for update sizes smaller or equal to the value of the target schedules and to $p(r^t = 1) = 0.1$ otherwise. This abrupt change of the success probabilities and the shape of the target schedules “constant” and “linear” are very unlike the behavior of the attacks during meta-training; nevertheless the empirical schedules by the controller follow the target behavior reasonably good, indicating that the learned square-size controller generalizes well.

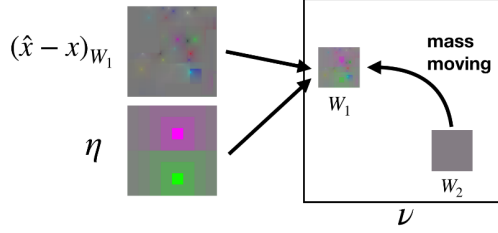


Figure 8: Perturbation of the ℓ_2 attack. Image source: Andriushchenko et al. [1]

A.5 Meta Square Attack for the ℓ_2 threat model

To meta-learn the update size controller for the ℓ_2 threat model we use the same procedure as discussed in Section 3.3. The only difference is the relaxation that we use to sample continuous updates since the update geometry is different. See Section A.3 for the ℓ_∞ case.

The sampling procedure of the ℓ_2 Square Attack is described in detail in the Algorithm 3 in Andriushchenko et al. [1]. On a high level the algorithm consists of 2 steps (Figure 8):

1. Take the mass from W_2
2. Update W_1

Let s be non-integer square size. $odd(s)$ – the largest odd integer number not exceeding s , $odd(s) = 2 \cdot \lfloor \frac{s-1}{2} \rfloor + 1$. The performed update is a linear interpolation between the squares of size $odd(s)$ and $odd(s) + 2$. We denote $frac(s) = \frac{s-odd(s)}{2} \in [0; 1)$ that will be an interpolation coefficient.

For the step 1 we consider the window W_2 of size $odd(s)$ and denote it's 1-pixel outer boundary as W_2^B . As in SA [1], we set the whole W_2 to 0 and add $\|W_2\|_2$ to the update budget. We also add $frac(s) \cdot \|W_2^B\|_2$ to the budget, therefore taking $frac(s)$ part of the norm. We update the boundary as $W_{2,new}^B := \sqrt{1 - frac(s)^2} \cdot W_2^B$. We get $\|W_2^B\|_2^2 = \|W_{2,new}^B\|_2^2 + frac(s)^2 \cdot \|W_2^B\|_2^2$.

A.6 Used data

In this work we only use the data published under formal licenses. To the best of our knowledge, data used in this project do not contain any personally identifiable information or offensive content.

For the CIFAR10 and CIFAR100 experiments in Table 8, we use pre-trained models from the RobustBench [28]. Information about architecture of the models and licenses of the corresponding model weights are in Table 11. Full texts of the licenses are available under the following link: <https://github.com/RobustBench/robustbench/blob/master/LICENSE>.

Table 11: Architecture and licenses of the models used in this work

Dataset	Model	Architecture	Model weights license
CIFAR10	Wong et al. [51]	ResNet-18	MIT
	Ding et al. [3]	WideResNet-28-4	Attribution-NonCommercial-ShareAlike 4.0 International; Copyright (c) 2020, Borealis AI
	Engstrom et al. [56]	ResNet-50	MIT
	Gowal et al. [62]	WideResNet-28-10	Apache License 2.0; Copyright (c) 2021, Google
	Carmon et al. [63]	WideResNet-28-10	MIT
	Huang et al. [52]	WideResNet-34-10	MIT
	Andriushchenko and Flammarion [64]	PreActResNet-18	MIT
	Zhang et al. [65]	WideResNet-34-10	MIT
	Hendrycks et al. [66]	WideResNet-28-10	Apache License 2.0; Copyright (c) 2019, Dan Hendrycks
	Wang et al. [67]	WideResNet-28-10	MIT
	Cui et al. [54]	WideResNet-34-10	MIT
	Sitawarin et al. [68]	WideResNet-34-10	MIT
	Wu et al. [53]	WideResNet-34-10	MIT
	Zhang et al. [69]	WideResNet-28-10	MIT
	Zhang et al. [70]	WideResNet-34-10	MIT
	Zhang et al. [71]	WideResNet-34-10	MIT
Rice et al. [61]	PreActResNet-18	MIT	
Augustin et al. [72]	ResNet-50	MIT	
Rony et al. [73]	WideResNet-28-10	BSD 3-Clause License; Copyright (c) 2018, Jerome Rony	
CIFAR100	Wu et al. [53]	WideResNet-34-10	MIT
	Cui et al. [54]	WideResNet-34-10	MIT
ImageNet	Salman et al. [55]	ResNet-18	MIT
	Engstrom et al. [56]	ResNet-50	MIT
	He et al. [58]	ResNet-50	BSD-3-Clause License (torchvision [74])
	Simonyan and Zisserman [59]	VGG16-BN	BSD-3-Clause License (torchvision [74])
	Szegedy et al. [60]	Inception v3	BSD-3-Clause License (torchvision [74])